

Effect of NiO spin orientation on the magnetic anisotropy of the Fe film in epitaxially grown Fe/NiO/Ag(001) and Fe/NiO/MgO(001)

Wondong Kim,^{1,2} E. Jin,¹ J. Wu,¹ J. Park,¹ E. Arenholz,³ A. Scholl,³ Chanyong Hwang,² and

Z. Q. Qiu¹

¹Department of Physics, University of California Berkeley, Berkeley, CA 94720

²Division of Industrial Metrology, Korea Research Institute of Standards and Science, 209 Gajeong-Ro, Yuseong-Gu, Daejeon 305-340, Korea

³Advanced Light Source, Lawrence Berkeley National Laboratory, Berkeley, CA 94720

Abstract

Single crystalline Fe/NiO bilayers were epitaxially grown on Ag(001) and on MgO(001), and investigated by Low Energy Electron Diffraction (LEED), Magneto-Optic Kerr Effect (MOKE), and X-ray Magnetic Linear Dichroism (XMLD). We find that while the Fe film has an in-plane magnetization in both Fe/NiO/Ag(001) and Fe/NiO/MgO(001) systems, the NiO spin orientation changes from in-plane direction in Fe/NiO/Ag(001) to out-of-plane direction in Fe/NiO/MgO(001). These two different NiO spin orientations generate remarkable different effects that the NiO induced magnetic anisotropy in the Fe film is much greater in Fe/NiO/Ag(001) than in Fe/NiO/MgO(001). XMLD measurement shows that the much greater magnetic anisotropy in Fe/NiO/Ag(001) is due to a 90°-coupling between the in-plane NiO spins and the in-plane Fe spins.

PACS numbers: 75.70.Ak

1. Introduction

Although an antiferromagnetic (AFM) material alone does not switch its spin direction within a magnetic field, the AFM layer could have a dramatic effect on a ferromagnetic (FM) layer in contact with it. For example, when cooling a FM/AFM bilayer system within a magnetic field from above to below the Neel temperature of the AFM layer, the FM layer hysteresis loop could shift in the applied magnetic field which is called exchange bias [1]. Even without field cooling, the AFM layer could induce a magnetic anisotropy in the FM layer to increase the FM layer coercivity [2]. These properties have been attributed to the unique character of FM/AFM interfacial interaction. Different from FM/FM interfacial interaction, the FM/AFM interfacial interaction is always accompanied by the so-called spin frustration that nearest neighbor coupling energy can not be minimized for all spin pairs at the same time. This characteristic property makes the FM/AFM bilayer system one of the most interesting and most intensively studied subject in nanomagnetism research.

Among many interesting phenomena related to the FM/AFM interfacial interaction, one fundamental issue is why and how the AFM layer induces a magnetic anisotropy in the FM layer. Phenomenally speaking, the AFM order breaks spatial rotational symmetry thus should in principle assign a magnetic anisotropy to the FM layer. Microscopically, however, it is not clear on how the FM/AFM interfacial interaction increases this magnetic anisotropy in the FM layer. Different mechanisms have been proposed to explain this phenomenon such as the spin flop coupling [3], local magnetic pinning centers [4], and the roughness-induced spin compensation [5], etc. In experiment, it is usually difficult to single out the exact effect of the AFM layer due to the difficulty of a direct measurement of the AFM spin structure and the difficulty of tuning the interfacial spin frustration. Regarding to the measurement, this difficulty is partially overcome by the recent development of X-ray Magnetic Linear Dichroism (XMLD) technique which could probe the spin direction in certain AFM thin films [6]. For example, it is now possible to directly measure the relative spin directions in some FM/AFM systems [7,8] and use the result to explain the abnormal interlayer coupling between two FM layers across an AFM layer [9]. Regarding to the tuning of the interfacial spin frustration, recent effort is on the controlling of the magnetic spin direction rather than on the interfacial roughness so that geometric frustration can be partially separated from the intrinsic spin frustration. For example, it was recently shown that by switching the Ni spin direction from out-of-plane to in-plane directions in a Ni/FeMn

bilayer, the Neel temperature of the FeMn layer could be changed by 60K without a change of the Ni/FeMn interfacial roughness [10]. This result demonstrates the importance of the FM spin orientation on the AFM properties. However, the reversed effect (e.g., the effect of the AFM spin orientation on the FM properties) has not yet been explored. We will address this issue in this work.

Among different FM/AFM bilayer systems, Fe/NiO(001) has emerged as a model system because of the epitaxial growth between Fe and NiO and the big XMLD signal from the AFM NiO film. Although there exists certain degrees of intermixing and structural bulking [11], Fe/NiO can be synthesized into single crystalline ultrathin films which is crucial to the XMLD measurement. In this paper, we report our study on epitaxially grown Fe/NiO bilayers. By growing a 20nm Ag(001) film on half of a MgO(001) substrate and the Fe/NiO bilayer on both the Ag(001) and MgO(001) at the same time, we realized Fe/NiO/Ag(001) and Fe/NiO/MgO(001) under the same growth condition of the Fe/NiO bilayer. As shown by XMLD measurement, although the Fe film has an in-plane magnetization in both systems, the NiO spin has an in-plane direction in Fe/NiO/Ag(001) and an out-of-plane direction in Fe/NiO/MgO(001). Consequently, the different NiO spin orientations have dramatic different effects on the Fe film magnetic properties that the in-plane NiO spins induce a much greater magnetic anisotropy in the Fe layer than the out-of-plane NiO spins.

2. Experiment

A 10×10mm square shaped MgO(001) single crystal disk was used as the substrate. After ultrasonic cleaning, the substrate was introduced into an ultra high vacuum chamber of base pressure of $1-2 \times 10^{-10}$ Torr, and then annealed at 600°C for ~10 hours. After this treatment, the MgO(001) substrate exhibits a sharp 1x1 Low Energy Electron Diffraction (LEED) pattern [Figure 1(a)], showing that a well-defined single crystalline surface has been formed. A 20 nm Ag film was deposited on half of the MgO(001) substrate at room temperature using a thermal evaporator by blocking half of the MgO substrate with a knife-edged shutter in front of the substrate. In this way, we have both Ag(001) and Mg(001) surfaces from the same 10×10mm substrate. The film was annealed at 150°C after the Ag growth to improve the surface smoothness. LEED pattern from the 20nm Ag [Fig. 1(b)] shows that single crystalline Ag(001) surface has been formed.

A NiO film was grown onto this half-Ag and half-MgO substrate at room temperature by evaporating Ni at $\sim 1 \text{ \AA}/\text{min}$ evaporation rate using a commercial electron-beam

evaporator under 1×10^{-6} Torr oxygen background pressure. The NiO film was grown into a wedge shape (0-30 ML) by moving the substrate behind the knife-edge shutter during the NiO growth. LEED measurement was taken again to check the structure of the NiO film [Fig. 1(c)-(d)]. As shown in the figure, the NiO film grown on both the Ag-covered part and the bare MgO(001) substrate shows well-ordered LEED spots, indicating an epitaxial growth of NiO on both Ag(001) and on MgO(001) substrates, in agreement with the literature result [12,13]. However, the LEED spots from NiO/Ag(001) is broader than that of NiO/MgO(001), showing that the NiO film surface is slightly rougher on NiO/Ag than on NiO/MgO although we couldn't provide a quantitative analysis. After pumping the vacuum chamber back to low 10^{-10} Torr, a uniform 8 ML Fe film was grown on top of the NiO wedge and checked by LEED [Fig. 1(e)-(f)] to ensure the formation of single crystalline Fe film. The sample was then covered by a 10 ML Ag to protect the film from contamination. Because both the NiO wedge and the Fe film were grown at the same time on both Ag and MgO, our sample provides a direct comparison on samples of Fe/NiO/Ag(001) and Fe/NiO/MgO(001) so that effect due to growth condition variation can be eliminated in our experiment.

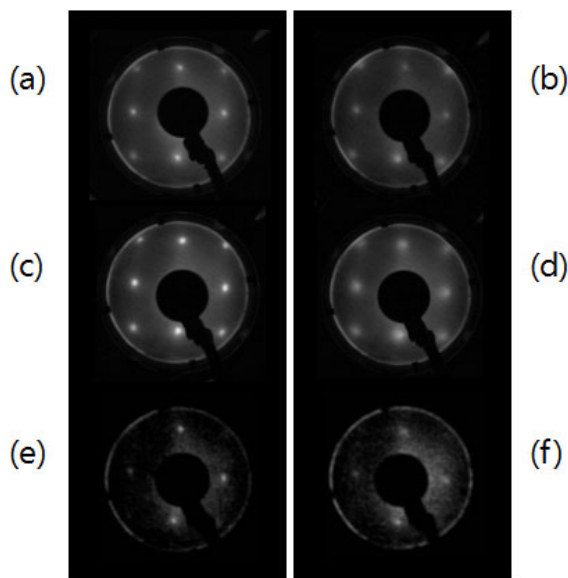


Figure 1: LEED patterns measured at 180 eV electron energy from (a) clean MgO(001), (b) Ag(20nm)/MgO(001), (c) NiO(30ML)/MgO(001), (d) NiO(30ML)/Ag(20nm)/MgO(001), (e) Fe(8ML)/NiO(30ML)/MgO(001) and (f) Fe(8ML)/NiO(30ML)/Ag(20nm)/MgO(001).

Magneto Optical Kerr Effect (MOKE) measurement was performed to obtain the Fe hysteresis loop as a function of the NiO thickness for both Fe/NiO/Ag(001) and Fe/NiO/MgO(001) along the NiO wedge. A He-Ne laser was used as the light source and a rotatable magnet applies a magnetic field to the film in both the in-plane and out-of-plane directions. X-ray Absorption Spectroscopy (XAS) and X-ray Magnetic Linear Dichroism (XMLD) measurements were performed at beamline 4.0.2 of the Advanced Light Source of Lawrence Berkeley National Laboratory. The incident x-ray has a $99\pm 1\%$ linear polarization. The linear polarization vector of the x-ray can be controlled by adjusting the gap of the elliptically polarized undulator at the beamline. XAS was obtained in total electron yield mode by measuring the sample current. The x-ray beam size is about $100\times 100\ \mu\text{m}$, which is estimated to cover only ~ 0.4 ML thickness range of the NiO wedge so that measurement at a given location of the NiO wedge can be regarded as a measurement from a uniformly thick NiO film.

3. Result and Discussion

The Fe hysteresis loops were measured at room temperature. No polar loops were detected showing that the 8ML Fe film has an in-plane magnetization in both Fe/NiO/Ag(001) and Fe/NiO/MgO(001) systems. Therefore we show only the Fe in-plane hysteresis loops in this paper. Fig. 2 shows the Fe in-plane hysteresis loops at different NiO thicknesses in both Fe/NiO/Ag(001) and Fe/NiO/MgO(001). The external magnetic field was applied in the NiO [110] axis direction, which is the Fe [100] easy magnetization axis of bcc Fe. Below 7ML NiO thickness, both Fe/NiO/Ag(001) and Fe/NiO/MgO(001) show a small coercivity (< 50 Oe). The small different coercivities of these two systems are attributed to either the different surface roughness of the NiO film as revealed by the LEED patterns in Fig. 1 or to the slight different NiO strains due to the different Ag and MgO lattice constants. As the NiO film thickness increases above 7ML, the coercivity of the Fe/NiO/Mg(001) film increases only slightly to ~ 75 Oe but the coercivity of the Fe/NiO/Ag(001) film increases drastically to as high as 375 Oe. We attribute this coercivity enhancement to the AFM order of the NiO layer above 7ML at room temperature. The coercivity enhancement of a ferromagnetic layer in contact with an AFM layer is a common phenomenon in FM/AFM systems. The AFM order should in principle induce an exchange bias and a magnetic anisotropy [2] to the FM layer. Since the Fe film in our sample was grown on top of the NiO layer and no field cooling was performed, we expect only an enhancement of the magnetic coercivity in our sample. We noticed that H_c has a peak at ~ 10 ML NiO and followed by a slow decrease with NiO

thickness in Fe/NiO/MgO(001). This result shows that there also exists Fe/NiO magnetic coupling. The peak behavior was reported in the literature [2] and has to come from the change of the Fe/NiO interfacial interaction. But it is unclear at this moment on whether it is due to the thickness dependent NiO magnetic anisotropy or the thickness dependent NiO spin orientation. Future studies are needed to resolve this issue.

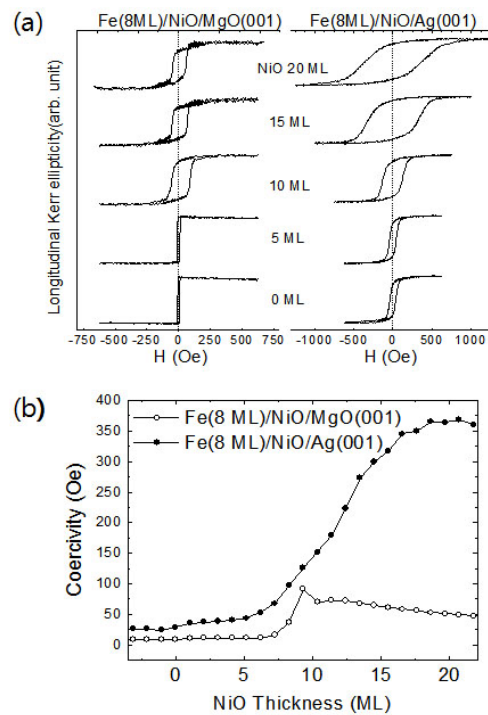


Figure 2: (a) Hysteresis loops and (b) coercivity of Fe(8ML)/NiO/Ag(001) and Fe(8ML)/NiO/MgO(001) at room temperature as a function of NiO thickness. The AFM order of the NiO film above 7ML NiO results in a much greater Fe coercivity enhancement in Fe/NiO/Ag(001) than in Fe/NiO/MgO(001).

The next question is why the coercivity enhancement occurs only above 7ML NiO. This is because the magnetic ordering temperature of a magnetic thin film depends on its film thickness due to the dimensionality effect. In fact, a reduction of the Curie temperature in FM thin films has been known for a long time [14]. Recent experiment on AFM films suggests that the Neel temperature of an AFM thin film is also reduced in ultrathin regime [15]. Therefore, the coercivity enhancement of the Fe film above 7ML NiO in our samples simply reflects the fact that the NiO film at room temperature is at

AFM state above 7ML but paramagnetic state below 7ML. To confirm this statement, we grow a new sample of Fe(8ML)/Ag(3ML)/NiO(12ML)/Ag(001) and performed temperature dependent measurement. The 3ML Ag is used to prevent intermixing between Fe and NiO at high temperature but to retain the Fe/NiO magnetic interaction. Fe hysteresis loops were taken at different temperatures. As shown Fig. 3, the coercivity of the sample decreases with increasing the temperature above the Neel temperature and is fully recovered after cooling down the sample to room temperature. This result proves that the coercivity enhancement shown in Fig. 2 above 7ML NiO is indeed due to the AFM order of the NiO layer.

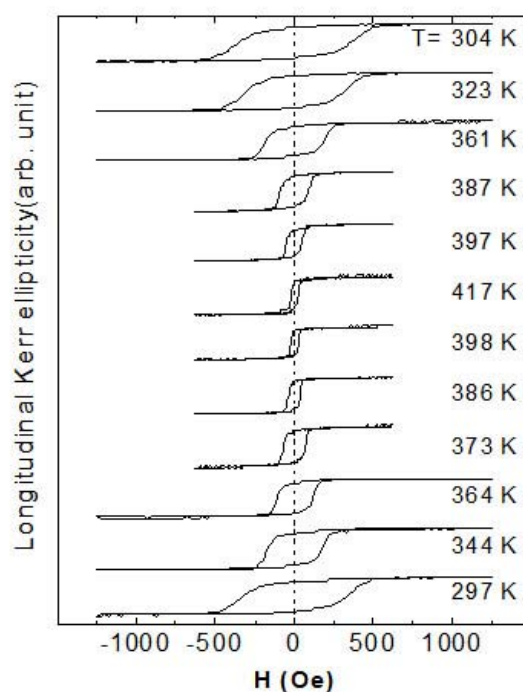


Figure 3: Temperature dependence of the Fe hysteresis loops of Fe(8ML)/Ag(3ML)/NiO(12ML)/Ag(001). The result proves that the Fe coercivity enhancement is due to the NiO antiferromagnetic order ($T_N=400$ K for 12 ML NiO).

The most remarkable result of Fig. 2 is that the coercivity enhancement of the Fe film in Fe/NiO/Ag(001) is much greater than that in Fe/NiO/MgO(001). This result can not be explained by the different film roughness or different Ag and MgO lattice constants because the coercivity difference between Fe/NiO/Ag and Fe/NiO/MgO below 7ML NiO is much smaller than the difference above 7ML NiO. Then the much greater

coercivity enhancement in Fe/NiO/Ag(001) than in Fe/NiO/MgO(001) must come from the different Fe/NiO magnetic interactions in these two systems, i.e., the AFM order of the NiO film in NiO/Ag(001) and NiO/MgO(001) must have induced different magnetic anisotropies in the Fe film. In our sample, both Fe/NiO/Ag(001) and Fe/NiO/MgO(001) have the same 8ML Fe FM layer and MOKE measurement shows the same magnitude of their hysteresis loops, thus the coercivity difference can not come from the different Fe magnetic moment in these two system. Regarding to the NiO layer, although the NiO magnetic property could in principle depend on the NiO growth condition (e.g., oxygen deficiency), the fact that the NiO wedge in our Fe/NiO/Ag(001) and Fe/NiO/Mg(001) was grown at the same time can safely rule out the different NiO growth conditions in these two samples. After ensuring the same Fe and NiO films in our Fe/NiO/Ag(001) and Fe/NiO/MgO(001), the only possibility for the different coercivity enhancement in these two systems is that the NiO film has different AFM spin structures in these two systems. In the following, we discuss the different NiO spin orientations in Fe/NiO/Ag(001) and Fe/NiO/MgO(001) systems.

Bulk NiO has the rock-salt crystal structure with its AFM order accompanied by a small rhombohedral distortion along a [111] direction. The Ni²⁺ spins are ferromagnetically aligned within each (111) plane and antiferromagnetically aligned between adjacent (111) planes with a total of 24 energetically degenerate domain orientations in a bulk NiO single crystal [16]. In thin films, however, the NiO spins are usually modified due to strains imposed by the substrate. In particular, NiO film grown on MgO(001) and Ag(001) exhibits an out-of-plane [13] and in-plane [17] spin directions, respectively. In fact, it was demonstrated that the NiO spin direction could even be manipulated between out-of-plane and in-plane directions in a MgO/NiO/Ag(001) sandwich [12], or within the film plane by a vicinal Ag(001) surface [15]. Then the interesting question is what's the NiO spin direction after covering the NiO/Ag(001) and NiO/MgO(001) with a 8ML Fe overlayer? This would be a trivial question if the Fe/NiO interfacial interaction has a collinear coupling. In that case, the in-plane Fe magnetization would obviously result in an in-plane NiO spin direction. However, it is well known that FM/AFM interfacial interaction could result in a 90°-coupling between the FM and AFM spins. Therefore even though it might be trivial for the NiO spins to remain in-plane direction in the Fe/NiO/Ag(001) system, it is unclear that if the NiO spin direction should remain in the out-of-plane direction in the Fe/NiO/MgO(001) system. To answer this question, we carried out XMLD measurement on Fe/NiO/Ag(001) and Fe/NiO/MgO(001).

Fig. 4 depicts the XMLD measurement result on the Ni L_2 edge of Fe/NiO(30 ML)/MgO(001). The polarization of the linearly polarized x-ray lies in the incident plane so that as the incident angle varies the XAS could pick up the out-of-plane component of the NiO spins. This is actually the measurement geometry in the literature to prove that NiO/MgO(001) has an out-of-plane spin direction [13]. As shown in Fig. 4, the XAS shows a typical double peak feature at the Ni L_2 absorption edge. The L_2 ratio R_{L_2} (defined as the lower energy peak intensity divided by the higher energy peak intensity) exhibits a strong polarization dependence at different incident angles with the well-known $\cos^2\theta$ -dependence reported for the NiO/MgO(001) system [13], showing that the NiO spin in the Fe/NiO/MgO(001) also has an out-of plane spin component.

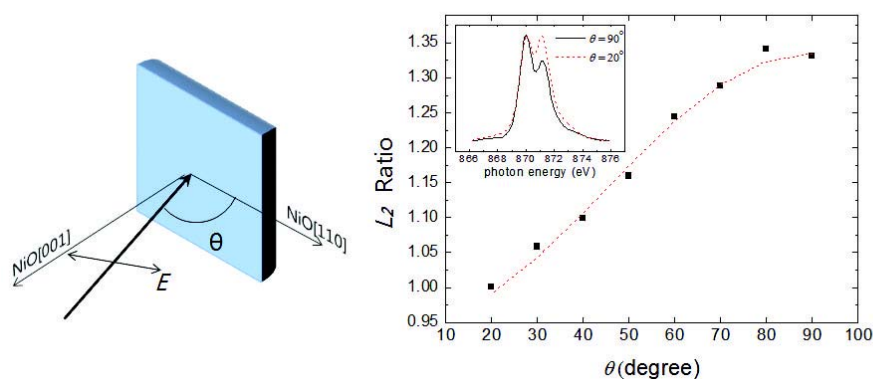


Figure 4: (Color online) Ni L_2 edge x-ray absorption spectra (inset) and the θ -dependence of the L_2 ratio of Fe(8ML)/NiO(30ML)/MgO(001). The $\cos^2\theta$ -dependence (dotted line) shows that the NiO spins have an out-of-plane component in the Fe(8ML)/NiO(30ML)/MgO(001).

To clarify the in-plane spin direction of the NiO film in the Fe/NiO/MgO(001), we performed the XMLD measurement at normal incidence but at different polarization angle (ϕ) of the linearly polarized x-ray (Fig. 5). In this way, a ϕ -dependent L_2 ratio would reflect the in-plane NiO spin component. The result shows that the Fe/NiO/MgO(001) has a negligible in-plane NiO spin component. In combination with the result of Fig. 4, we conclude that the NiO in Fe/NiO/MgO(001) film has an out-of-plane spin direction. In contrast, the L_2 ratio of Fe/NiO/Ag(001) at normal incidence of the x-ray shows a clear $\cos^2\phi$ dependence (Fig. 5). After switching the Fe magnetization by an external magnetic field from the NiO $[110]$ to $[1\bar{1}0]$ directions, the Ni L_2 ratio is revised accordingly (Fig. 5). This result shows that the NiO spins in Fe/NiO/Ag(001) have an in-plane direction as in the NiO/Ag(001) system. We also

carried out the XMLD measurement for thinner NiO films and observe the same results down to ~ 10 ML NiO below which the XMLD signal is too weak to determine the spin direction. We then determined the in-plane NiO spin direction relative to the Fe magnetization direction. Fig. 5 shows a $\cos^2\phi$ dependence of the L_2 ratio with the minimum/maximum values occurring at $\phi=0^\circ$ (NiO[110] axis) and $\phi=90^\circ$ (NiO[1 $\bar{1}$ 0] axis). This result shows that the NiO spin direction is along the NiO [110] or [1 $\bar{1}$ 0] axis. For NiO spin direction in the [110] axis, the L_2 ratio should reach maximum value as the x-ray polarization direction is parallel to the NiO spin axis, opposite to the [100] NiO easy axis case where the L_2 ratio reaches its minimum value as the x-ray polarization direction is parallel to the NiO spin axis [18,19]. Then the result of Fig. 5 shows that the in-plane NiO spins have a 90° -coupling to the Fe spins in the Fe/NiO/Ag(001) sample. In addition, the NiO spins rotate by 90° after the Fe magnetization is switched by 90° , i.e., the NiO spins are locked to the Fe spins to rotate together with the Fe spins.

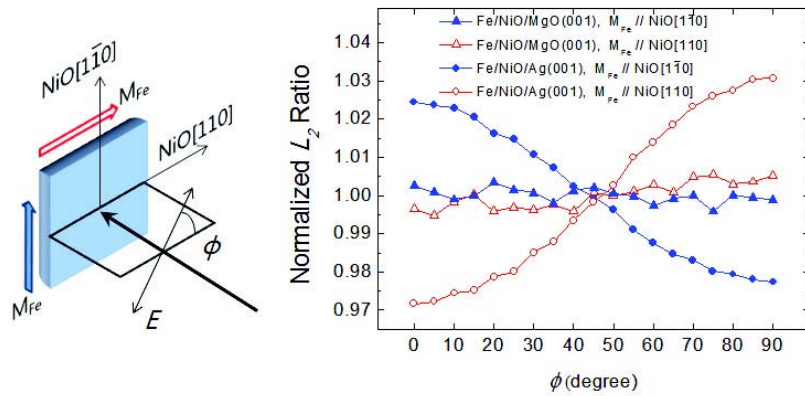


Figure 5: (Color online) Ni L_2 ratio at normal incidence of the x-rays from Fe(8ML)/NiO(30ML)/Ag(001) and Fe(8ML)/NiO(30ML)/MgO(001). The Fe magnetization is aligned by an external field to the NiO [1 $\bar{1}$ 0] (filled symbols) and NiO [110] directions (hollow symbols), respectively during the measurement. The result shows that the NiO spins in Fe(8ML)/NiO(30ML)/Ag(001) is in the film plane and 90° coupled to the Fe magnetization, and that the NiO spins in Fe(8ML)/NiO(30ML)/MgO(001) is in the out-of-plane direction.

The XMLD measurement clearly shows that the NiO layer has different spin orientations in Fe/NiO/Ag(001) and Fe/NiO/MgO(001) systems. This result explains the hysteresis loop result that the Fe coercivity in Fe/NiO/Ag(001) is much greater than that

in Fe/NiO/MgO(001). For the case of Fe/NiO/MgO(001), the NiO spins are in the out-of-plane direction so that as the Fe spins are rotated in the film plane by an external magnetic field, the NiO spins are not changing their directions thus will not add additional magnetic anisotropy to the Fe film. That is why the Fe coercivity in the Fe/NiO/MgO(001) changes so little as the NiO establishes AFM order above 7ML thickness. However, the 90°-coupling between Fe and NiO should tilt the Fe and NiO spins a tiny bit to produce a small parallel component of the NiO spins in the Fe spin direction. Although this tiny parallel component is beyond the XMLD measurement limit, we believe it accounts for the small increase of the Fe coercivity in the Fe/NiO/MgO(001) above 7ML NiO thickness. For the case of the Fe/NiO/Ag(001), the XMLD result shows that the NiO spins are in the film plane and are 90° coupled to the Fe spins. Therefore, as the Fe spins are rotated by an external magnetic field, the Fe/NiO coupling also drags the NiO spins to rotate together with the Fe magnetization so that the Fe spins should carry the effect of the NiO magnetic anisotropy during its magnetization reversal, leading to a much greater Fe coercivity than that generated by the Fe magnetic anisotropy alone. This explains the Fe/NiO/Ag(001) result that the Fe coercivity is greatly enhanced after the NiO film establishes AFM order above 7ML thickness. It should be mentioned that the NiO spins in the Fe/NiO/MgO(001) should be tilted away from the surface normal direction due to the Fe/NiO interfacial interaction. To make a rough estimation of the NiO tilting angle, we make an over simplified assumption that the coercivity enhancement is entirely determined by the in-plane NiO component for both Fe/NiO/MgO(001) and Fe/NiO/Ag(001). Under this assumption, the ratio of the coercivity enhancement for these two cases would give the tilting angle $\tan\alpha \sim \Delta H_c(\text{Fe/NiO/MgO})/\Delta H_c(\text{Fe/NiO/Ag}) \sim 50/350 = 0.14$ or $\alpha \sim 8^\circ$. This is only a rough estimation because other factors such as roughness and strain are not considered.

4. Summary.

We investigated Fe/NiO/Ag(001) and Fe/NiO/MgO(001) using MOKE and XMLD techniques. Although the Fe film in both systems has an in-plane magnetization, XMLD measurement shows that the NiO spins are in the film plane in the Fe/NiO/Ag(001) and out-of-plane in the Fe/NiO/MgO(001). In addition, the in-plane NiO spins in the Fe/NiO/Ag(001) are 90° coupled to the Fe magnetization to rotate together with the Fe magnetization. This result explains the Fe hysteresis loop measurement that as the NiO thickness increases to establish its antiferromagnetic order, the Fe coercivity is greatly enhanced in Fe/NiO/Ag(001) while only slightly enhanced in Fe/NiO/MgO(001).

Therefore we conclude that the in-plane NiO spins have a much stronger effect on the in-plane Fe magnetic anisotropy than the out-of-plane NiO spins.

Acknowledgement

This work was supported by National Science Foundation DMR-0803305, U.S. Department of Energy DE-AC02-05CH11231, and KICOS through Global Research Laboratory project.

References:

1. W. H. Meiklejohn and C. P. Bean, *Phys. Rev.* **102**, 1413 (1956).
2. J. Nogués and Ivan K. Schuller, *J. of Magn. Mag. Mat.* **192**, 203 (1999).
3. N. C. Koon, *Phys. Rev. Lett.* **78**, 4865 (1997).
4. W. Kuch, F. Offi, L. I. Chelaru, M. Kotsugi, K. Fukumoto, and J. Kirschner, *Phys. Rev. B* **65**, 140408 (2002).
5. J. Wu, J. Choi, A. Scholl, A. Doran, E. Arenholz, Chanyong Hwang, and Z. Q. Qiu, *Phys. Rev. B* **79**, 212411 (2009).
6. A. Scholl, J. Stöhr, J. Lüning, J. W. Seo, J. Fompeyrine, H. Siegart, J.-P. Locquet, F. Nolting, S. Anders, E. E. Fullerton, M. R. Scheinfein, H. A. Padmore, *Science* **287**, 1014 (2000).
7. H. Ohldag, T. J. Regan, J. Stöhr, A. Scholl, F. Nolting, J. Lüning, C. Stamm, S. Anders, and R. L. White, *Phys. Rev. Lett.* **87**, 247201 (2001).
8. M. Finazzi, A. Brambilla, P. Biagioni, J. Graf, G.-H. Gweon, A. Scholl, A. Lanzara, and L. Duò, *Phys. Rev. Lett.* **97**, 097202 (2006).
9. J. Wu, J. Choi, A. Scholl, A. Doran, E. Arenholz, Y. Z. Wu, C. Won, Chanyong Hwang, and Z. Q. Qiu, *Phys. Rev. B* **80**, 012409 (2009).
10. K. Lenz, S. Zander, and W. Kuch, *Phys. Rev. Lett.* **98**, 237201 (2007).
11. P. Luches, V. Bellini, S. Colonna, L. Di Giustino, F. Manghi, S. Valeri, and F. Boscherini, *Phys. Rev. Lett.* **96**, 106106 (2006).
12. S. Altieri, M. Finazzi, H. H. Hsieh, H. -J. Lin, C.T. Chen, T. Hibma, S. Valeri, and G. A. Sawatzky, *Phys. Rev. Lett.* **91**, 137201 (2003).
13. D. Alders, L. H. Tjeng, F. C. Voogt, T. Hibma, G. A. Sawatzky, C. T. Chen, J. Vogel, M. Sacchi, and S. Iacobucci, *Phys. Rev. B* **57**, 11623 (1998).
14. Renjun Zhang and Roy F. Willis, *Phys. Rev. Lett.* **86**, 2665 (2001).
15. Y. Z. Wu, Y. Zhao, E. Arenholz, A. T. Young, B. Sinkovic, C. Won, and Z. Q. Qiu, *Phys. Rev. B* **78**, 064413 (2008).
16. F. Keffer and W. O'Sullivan, *Phys. Rev.* **108**, 637 (1957).

-
17. D. Spanke, V. Solinus, D. Knabben, F. U. Hillebrecht, F. Ciccacci, L. Gregoratti, and M. Marsi, Phys. Rev. B **58**, 5201 (1998).
 18. Elke Arenholz, Gerrit van der Laan,, Rajesh V. Chopdekar, and Yuri Suzuki, Phys. Rev. Lett. **98**, 197201 (2007).
 19. I. P. Krug, F. U. Hillebrecht, M. W. Haverkort, A. Tanaka, L. H. Tjeng, H. Gomonay, A. Fraile-Rodríguez, F. Nolting, S. Cramm, and C. M. Schneider, Phys. Rev. B **78**, 064427 (2008).